

The influence of Coulomb interaction on transport through mesoscopic two-barrier structures

Wolfgang Häusler, B. Kramer, J. Mašek

Angaben zur Veröffentlichung / Publication details:

Häusler, Wolfgang, B. Kramer, and J. Mašek. 1991. "The influence of Coulomb interaction on transport through mesoscopic two-barrier structures." *Zeitschrift für Physik B Condensed Matter* 85 (3): 435–42. <https://doi.org/10.1007/bf01307641>.

Nutzungsbedingungen / Terms of use:

licgercopyright

Dieses Dokument wird unter folgenden Bedingungen zur Verfügung gestellt: / This document is made available under these conditions:

Deutsches Urheberrecht

Weitere Informationen finden Sie unter: / For more information see:

<https://www.uni-augsburg.de/de/organisation/bibliothek/publizieren-zitieren-archivieren/publiz/>



The influence of Coulomb interaction on transport through mesoscopic two-barrier structures

W. Häusler¹, B. Kramer¹, and J. Mašek²

¹ Physikalisch-Technische Bundesanstalt Braunschweig, Bundesallee 100, W-3300 Braunschweig, Federal Republic of Germany

² Institute of Physics, Prague, CSFR

We investigate the influence of the Coulomb interaction on the energy spectrum of a finite number of electrons in a geometrically confined quantum mechanical system. The spectrum is calculated numerically using the Slater determinants of the one-electron states as basis set. It is found to be dominated by the Coulomb repulsion when the system is large. Coulomb and exchange matrix elements for a given combination of four one-electron states are of the same order of magnitude. As a consequence, the energy difference between the ground states of the $(N+1)$ - and the N -electron system is an order of magnitude smaller than each of the matrix elements, although being much larger than the separation of the one-electron energy levels. We discuss the importance of the interaction effects for the explanation of the recently observed resonant behavior of the electronic transport through quantum dots.

1. Introduction

The transfer of charge carriers through small systems, like narrow electronic channels in semiconductors, at low temperatures, reveal a rich variety of new and surprising quantum phenomena, due to the quantization of the energy levels and the coherence of the corresponding one-particle quantum states. Quantization of the conductance, quantum interference oscillations, and universal conductance fluctuations are frequently discussed examples [1]. Small quantum island formed by two narrow constrictions in series, exhibit another most striking phenomenon, namely pronounced regular, periodic oscillations of the conductance when the voltage applied to a suitably shaped metallic gate is changed [2]. The behavior of these resonances with varying gate voltage, and an applied magnetic field, suggested that besides one-electron quantization Coulomb interaction between the electrons is one of the dominant effects that have to be taken into account for a proper understanding of the experiment [3].

That Coulomb interaction can lead to striking effects in the transport properties of small structures was already anticipated by theoretical considerations concerning the Coulomb blockade of the tunneling of single electrons through small tunnel junctions [4]. The corresponding non-linearity of the current-voltage characteristics was recently experimentally detected. The realization of the so-called turnstile device, a single-electron counter that can be used to construct an electrical current standard, is based on this effect [5].

The theoretical understanding of transport processes in quantum mechanically coherent systems was pioneered in the seventies by Landauer [6]. The basic idea of this approach was that quantum DC-transport is closely related to quantum mechanical, coherent tunneling of the charge carriers from one reservoir of carriers to another. Starting from quantum mechanical linear response theory for independent particles the relation between the DC-conductance and the quantum transmission probability was formally established [7, 8]. Dissipative processes, a consequence of the couplings of the charge carriers between themselves, and to external degrees of freedom, were assumed to be absent from the regions where the tunneling processes actually take place. Dissipation and equilibration were supposed to occur only in the reservoirs [9]. A definition of the conductance solely in terms of properties of the "sample", and independent of the spatial behavior of the applied electric field turned out to be only possible in the DC-limit [10], since the conductivity in the coherent regime is intrinsically non-local [11].

The non-interacting electron picture, within linear response theory, is able to explain many of the observed transport phenomena in mesoscopic structures. However, there were theoretical predictions [12], and also experimental indications [13] that non-linear effects are important even if the electron-electron interaction does not dominate. When Coulomb interaction becomes important, non-linear effects like the Coulomb blockade dominate the transfer of charges through small systems. The theoretical understanding of the phenomena in this

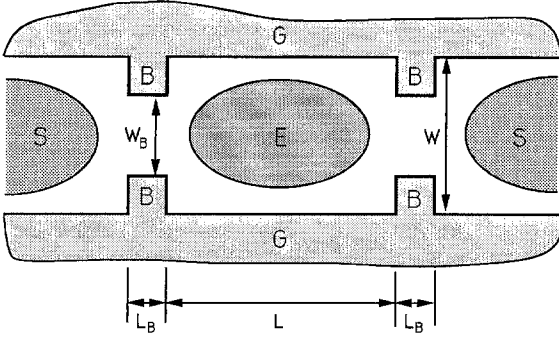


Fig. 1. Schematic view of the gate configuration (*G*) on top of a AlGaAs/GaAs heterostructure that can be used to realize an almost isolated island of electrons (*E*) between two potential barriers (*B*) that are electro-statically defined by a voltage applied between the gate and the AlGaAs/GaAs substrate underneath. Although the geometry of the gate determines the spatial size of the electron island, the true shape of the latter is not directly given by the geometrical shape of the former. The confining potential must be determined from a self-consistent calculation taking into account the changes in the distribution of the electrons in the inversion layer when the gate voltage is applied. The electron island is coupled quantum mechanically to semi-infinite quasi-one dimensional electron systems (*S*) via tunneling through the barriers

regime has matured considerably during the past years [14]. Whether, and to what extent, Coulomb interaction is also important for linear transport was not clear until the above mentioned experimental discovery of the oscillatory behavior of the (linear) conductance of two quantum mechanical point contacts in series (Fig. 1). The observation that the conductance peaks do not split when a magnetic field is applied indicate the absence of spin degeneracy. Since other mechanisms can be excluded in these semiconductor systems, this must be taken as a strong indication for the influence of electron correlation. Consequently, the linear theory for the transport properties, which in its simplest version neglects interactions, must be reformulated in order to be capable of treating the transport in the mesoscopic regime adequately. A first attempt in this direction that was based on a simple Hubbard like Hamiltonian for a single impurity connected to ideal metallic leads was made only recently [15].

The formulation of the transport theory including interactions requires some knowledge of the properties of the multi-electron states. Since the number of the physically relevant degrees of freedom in a mesoscopic system is limited, it is possible to obtain accurate results on the multi-electron states that are of direct experimental relevance. There were successful attempts to diagonalize numerically N electron systems ($N \approx 10$) in the presence of Coulomb interaction, and a strong magnetic field in connection with the fractional quantum Hall effect [16]. Two coulombically interacting electrons in a parabolic confining potential in the presence of a magnetic field were considered by various authors [17, 18]. The Hubbard model was treated numerically already in 1979 [19].

The present paper is a report on similar calculations for a finite quasi-one dimensional system. In addition,

an attempt will be made to understand the recent experimental data [3, 20] using the results.

The structure of the paper is as follows. The results of extensive numerical calculations of the linear conductance of the geometry shown in Fig. 1, including the effects of moderate disorder, and a weak magnetic field, are described in the subsequent section. The resonant character of the tunneling through the two constrictions, due to the quasi-discreteness of the states within the island, is demonstrated. Section 3 describes our calculations for the interacting confined system. The results are presented in Sect. 4. Their consequences for the understanding of the experimental data are discussed in the Sect. 5.

2. Resonant electron transport

In this section, we discuss the results for the linear conductance within the non-interacting electron picture.

2.1. Model and method

The calculation of the DC-conductance was done by using the numerical recursive method that was derived earlier for the computation of the zero-temperature electronic properties of random systems with arbitrary geometry [10, 21].

The model consists of the discrete tight-binding Hamiltonian with diagonal matrix elements ε_j and constant nearest neighbor hopping matrix elements V ,

$$H = \sum_j \varepsilon_j |j\rangle \langle j| + V \sum_{j,j'} |j\rangle \langle j'|. \quad (1)$$

$\{|j\rangle\}$ denote the sites of a square lattice (lattice constant $a=1$), and $\{|j\rangle\}$ the corresponding basis states. The boundary of a system can be simulated by assuming $V=0$ between neighboring sites at the boundary. Alternatively, one can set $\varepsilon_j = \infty$ at the respective sites, in order to model an infinitely high potential wall. Disorder is modelled by taking ε_j as independent random variables constantly distributed in the interval $[-\Gamma/2, \Gamma/2]$ inside the region between the constrictions (*E* in Fig. 1). The influence of a magnetic field was investigated by using the Peierls substitution for the off-diagonal matrix elements [22]

$$V_{lm,l'm'}(B) = V \{ e^{\pm 2\pi i \alpha l} \delta_{l,l'} \delta_{m \pm 1, m'} + \delta_{l \pm 1, l'} \delta_{m, m'} \}, \quad (2)$$

where the parameter $\alpha \equiv eB/h$ is the number of the magnetic flux quanta within one unit cell.

In the calculations the width of the quasi-one dimensional system, W , was fixed to $11a$. The separation of the openings of the constrictions was $W_B = 7a$, their length varying between $L_B = 5a$ and $L_B = 20a$. The barriers were modelled by taking $\varepsilon_j = 10V$ at the respective lattice positions (regions *B* in Fig. 1). The distances between the contacts were $L = 50a, 100a$, and $200a$. The total length of the system including the leads *S* attached to both sides was assumed to be infinite. Inside the system, $\varepsilon_j = 0$ without disorder.

2.2. Results for the conductance

The result for the conductance as a function of the Fermi energy for $L=200$ is shown in Fig. 2 together with the conductance of a single constriction. The tight-binding band edge of the infinite system is at $-4V$. Due to the confinement in the W -direction the first quasi-one dimensional subband starts at a somewhat higher energy $E_0 \approx (-4 + (\pi/W)^2)V \approx -3.92V$ for the width considered here. At this energy the conductance is dominated by tunneling, and grows exponentially for the single constriction. In the case of the two constrictions in series there are pronounced resonances at the energies of the quasi-bound states corresponding to the region between the two contacts. The conductance saturates at the onset of the lowest subband of the infinite quasi-one dimensional system with $W_B = 7a$, the width of the constrictions ($E_1 = -3.80V$). For perfect confinement the energetic distance between the (in this case δ -function like) resonances is given by $\Delta E \approx 2\pi\sqrt{(E-E_0)/L}$. The quantum mechanical coupling between the interior of the island between the barriers to the semi-infinite quantum wires on both sides via tunneling leads to the finite width of the resonances. This is shown in the inset of the Fig. 2 where we have plotted the peak widths as a function of the conductance of the single barrier, τ_1 . The linear dependence of the energetic peak width on τ_1 demonstrates the resonant tunneling character of the conductance, and the equivalence of linear response and Landauer formulations of the DC-conductance.

For comparison with the experiment we show in Fig. 3 results for $L=50a$, $100a$, $200a$ as a function of the charge density in the system. The latter is given by the integrated density of states of the total system, including the regions outside of the island. Near the band edge of the lowest subband the density of states has an $E^{-1/2}$ -van Hove singularity. The charge density is therefore proportional to the square root of E , and the peaks become exactly equidistant as a function of the charge density, their separation being $\propto L^{-1}$ (Fig. 3 inset).

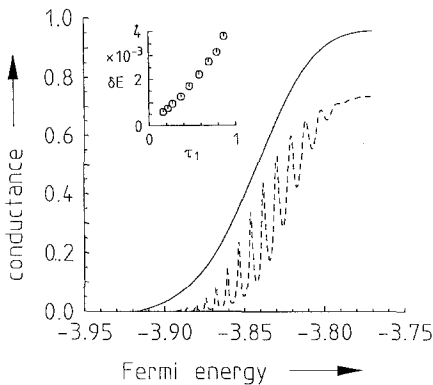


Fig. 2. Conductance of a quantum wire with two constrictions at $T=0$ as a function of the Fermi energy (dashed curve). The distance of the constrictions is $L=200a$. The full curve shows the conductance of a single constriction. The inset shows the width of the peaks, δE as a function of the conductance of the single constriction, τ_1 , at the position of the peaks

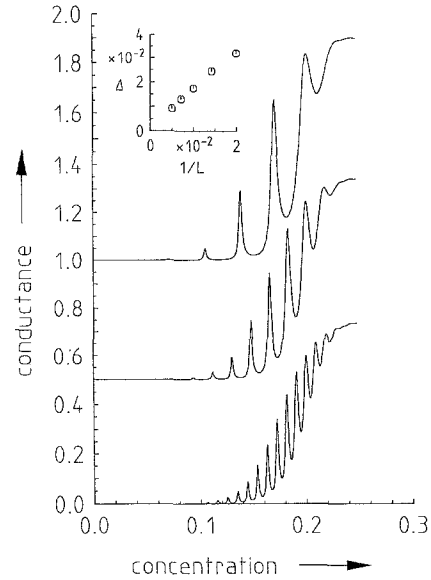


Fig. 3. Resonant tunneling conductance as a function of the electron concentration normalized to the area of W unit cells for $L=200a$ (lower curve), $L=100a$ (middle curve), and $L=50a$ (upper curve). The inset shows the dependence of the distance between the peaks as a function of L^{-1}

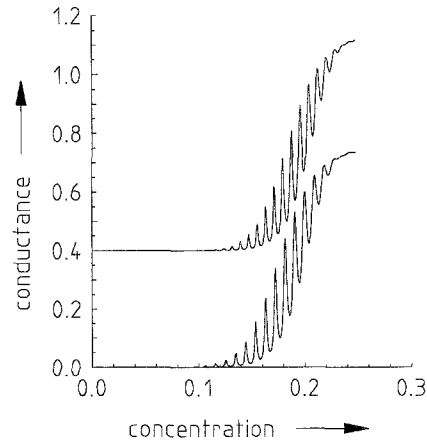


Fig. 4. The conductance as a function of the charge density for $\alpha=0$ (lower curve), and $\alpha=0.05$ (upper curve). The system was $L=200a$, $W=11a$, and $L_B=10a$

Taking into account a magnetic field ($\alpha=0.05$) does not change the conductance except for a slight shift of the positions of the resonances to higher densities resulting in somewhat smaller distances between the peaks (Fig. 4). These effects can be treated quantitatively by using perturbation theory. Including the electron spin would lead in addition to a constant Zeeman splitting of each of the peaks which is not included in the figure.

2.3. Comparison with experiment

Comparing the results shown so far with the experimental data for the conductance as a function of the gate voltage [3] an explanation in terms of a resonant tunneling model looks appealing. If we assume that the gate

voltage is proportional to the charge density, it explains qualitatively (i) the equidistance of the resonances, (ii) the dependence of the distance between the conductance peaks on the separation between the two barriers, and (iii) the fact that the width of the experimentally observed peaks is independent of the peak position (Fig. 3). Since the resonant tunneling picture predicts a finite peak width at $T=0$ (Fig. 2) it would also explain why the observed temperature dependence of the widths of the peaks saturates at low temperatures, although this effect may at least partially be attributed to electron heating caused by the absence of sufficient coupling to phonons.

There are, however, several features in the experiment that cannot be understood. First of all, there is the absence of Zeeman splitting when a moderate magnetic field is applied to the system. This indicates that the resonant states that are assumed to be responsible for the occurrence of the sharp conductance resonances cannot be occupied by two electrons with opposite spin as one would expect from the simple picture of noninteracting particles. Secondly, an analysis of the relation between the gate voltage and the charge added to the island leads to the conclusion that exactly one electron has to be added in order to generate a new conductance peak [3]. This is again a strong indication that the resonant states can only be singly occupied. Thirdly, the energetic distance between the conductance peaks deduced from the experiment was about 0.5 meV. This appears to be roughly an order of magnitude larger than the energetic distance between the one-electron resonances determined by using the effective mass for GaAs ($m=0.067 m_0$), and the distance between the two constrictions from the experiment ($L \approx 0.5 \mu\text{m}$). It is also claimed that there must be about 10^2 electrons on the island between the constrictions before the resonances in the conductance can be observed.

These observations indicate that the resonant one-electron picture alone is not sufficient for the understanding of the experiment, and that interaction effects are of importance. Since spin-orbit interaction is negligibly small near the conduction band edge in GaAs, it seems unavoidable to consider Coulomb interaction as one of the dominant physical mechanisms that are tested in this experiment.

3. Confined electron states in the presence of Coulomb interaction

In this section we investigate numerically in some detail the properties of the energy spectrum of N interacting electrons ($N \leq 6$) confined within a one dimensional square well potential of a finite height. However, in the presently considered context the height can be regarded as infinite. Main emphasis will be on the behavior of the ground state when the number of the electrons is changed.

3.1. The model

The Hamiltonian of the system is written in “atomic units” as

$$H = E_H \frac{a_0}{L} \left(\frac{a_0}{L} H_0 + H_I + H_b \right). \quad (3)$$

$E_H = \alpha^2 m c^2 = (27.2 m/m_0) \text{ eV}$ is the Hartree energy, $a_0 = \hbar^2/m e^2 = (0.529 m_0/m) \text{ \AA}$ the Bohr radius of an electron with the effective mass m , $\alpha = 1/137$ the Sommerfeld fine structure constant, and c the velocity of light.

$$H_0 = \sum_{n,\sigma} \varepsilon_n c_{n\sigma}^\dagger c_{n\sigma} \quad (4)$$

denotes the kinetic energy, and

$$H_I = \sum_{n_1 \dots n_4, \sigma_1, \sigma_2} V_{n_4 n_3 n_2 n_1} c_{n_4 \sigma_1}^\dagger c_{n_3 \sigma_2}^\dagger c_{n_2 \sigma_2} c_{n_1 \sigma_1} \quad (5)$$

the Coulomb interaction. $c_{n\sigma}^\dagger, c_{n\sigma}$ are creation and annihilation operators for the occupation of the n -th one-electron state ($n \geq 1$) of the square well of length L with an electron of spin σ , ε_n are the respective one-electron eigenvalues (corresponding approximately to the wave numbers $k_n = n\pi/2$ when the well is very high).

$$H_b = -N \sum_{n_4, n_1, \sigma} V_{n_4 1 1 n_1} c_{n_4 \sigma}^\dagger c_{n_1 \sigma} \quad (6)$$

is the contribution of the positively charged background. This contribution to the total energy was taken into account in some of the calculations, in order to get an insight into the possible influence of charge re-distribution on the energy spectra. For the matrix elements of the background potential we used for simplicity a spatial dependence of the charge density that corresponds to a positively charged non-interacting electron ground state wave function. The interaction with the background charge guarantees the extensivity of the ground state energy for different particle numbers N . For low electron densities this property does not depend on the details of the background charge distribution.

The form of the Hamiltonian displays explicitly the fact that the length of the system determines the relative importance of kinetic and Coulomb energy, when the background is neglected. It is only if $a_0/L \geq 1$ that the Coulomb energy can be expected to be negligible when compared with the one-electron level distances. Including the background, the critical parameter is $N a_0/L$ [23].

For the interaction energy we assume the Löwdin form [24]

$$V(x, x') \propto \frac{1}{\sqrt{(x-x')^2 + \lambda^2}}. \quad (7)$$

$\gamma = \lambda/L$ is a measure for the relative width of the electronic wave functions in the transversal direction. For $\gamma \leq 0.05$ the ground state energy is independent of γ although the individual matrix elements $V_{n_4 n_3 n_2 n_1}$ are increasing when γ decreases, as we will see later. In most of our calculations we used $\gamma = 2 \cdot 10^{-4}$.

Due to the symmetry of the potential, and the one-electron wave functions, the Coulomb matrix elements

$V_{n_4 n_3 n_2 n_1}$ are only non-vanishing if $\sum_{i=1}^4 n_i$ is even. Further-

more, they obey symmetry relations of the type

$$V_{n_4 n_3 n_2 n_1} = V_{n_4 n_2 n_3 n_1} = V_{n_1 n_3 n_2 n_4} = V_{n_3 n_4 n_1 n_2}. \quad (8)$$

For $\gamma \ll 1$ the Coulomb matrix elements can be written as

$$V_{n_4 n_3 n_2 n_1} = -8\pi \int_0^\infty dq (\ln(\gamma q) + C) \hat{f}_{14}(q) \hat{f}_{23}(-q). \quad (9)$$

\hat{f}_{ij} is the Fourier transform of the product $\varphi_{n_i}^*(x) \varphi_{n_j}(x)$ of the one-electron eigenfunctions φ_n of H_0 , and $C = 0.577$ the Euler constant.

3.2. Two electrons in two one-electron states

As a simple example, which nevertheless demonstrates essential physical properties of the interacting system, we consider two electrons that occupy two one-particle states.

The complete basis set consists of six ortho-normalized two particle Slater determinants. Four of them contain anti-parallel electron spins, $|S_1\rangle = |1\uparrow 1\downarrow\rangle$, $|S_2\rangle = |2\uparrow 2\downarrow\rangle$, $|S_3\rangle = |1\uparrow 2\downarrow\rangle$, $|S_4\rangle = |2\uparrow 1\downarrow\rangle$, two contain parallel spins, $|T_1\rangle = |1\uparrow 2\uparrow\rangle$, and $|T_2\rangle = |1\downarrow 2\downarrow\rangle$.

The matrix elements of the kinetic energy, Eq. (4), are

$$\langle v\sigma\mu\tau | H_0 | v'\sigma'\mu'\tau' \rangle = \delta_{vv'} \delta_{\mu\mu'} \delta_{\sigma\sigma'} \delta_{\tau\tau'} (\varepsilon_v + \varepsilon_{\mu}) \quad (10)$$

where $v, v', \mu, \mu' = 1, 2$ and $\sigma, \sigma', \tau, \tau' = \uparrow, \downarrow$. There are three different Coulomb-type matrix elements

$$\langle S_i | H_I | S_i \rangle = V_{iiii} \equiv U_{ii} \quad (i = 1, 2), \quad (11)$$

$$\langle S_j | H_I | S_j \rangle = V_{1221} \equiv U_{12} \quad (j = 3, 4), \quad (12)$$

and an exchange matrix element $A \equiv V_{1212}$ so that

$$\langle T_i | H_I | T_i \rangle = U_{12} - A \quad (i = 1, 2). \quad (13)$$

The only non-vanishing off-diagonal elements are

$$\langle S_1 | H_I | S_2 \rangle = \langle S_3 | H_I | S_4 \rangle = A. \quad (14)$$

U_{ij} and A are the Coulomb and exchange integrals of $V(x, x')$ with the one-electron wave functions. The contribution of a constant background charge density would be proportional to the unit matrix. It can be discarded.

The eigenvalues are easily calculated. One obtains

$$E_{1,2} = \varepsilon_1 + \varepsilon_2 + \frac{U_{11} + U_{22}}{2} \pm A \sqrt{1 + \frac{(\varepsilon_2 - \varepsilon_1 + (U_{22} - U_{11})/2)^2}{A^2}} \quad (15)$$

$$E_{3,4} = \varepsilon_1 + \varepsilon_2 + U_{12} \pm A \quad (16)$$

$$E_{5,6} = \varepsilon_1 + \varepsilon_2 + U_{12} - A \quad (17)$$

The triply degenerate state at $E_0 \equiv E_{4,5,6}$ is the ground state. It corresponds to a total spin of $S = 1$. The energy required to add the second electron to the system, given by the distance between the ground state energy of the two electrons, and the lowest one-electron state, is $\varepsilon_2 + U_{12} - A$, the difference between the Coulomb and the

exchange matrix elements if ε_2 is small. The compensation between Coulomb and exchange terms constitutes one of the most important features of the more general case of the system of N interacting electrons, as will be discussed below.

3.3. Some computational details

In this section we provide some of the technical details of the computation.

Since we are interested only in the lowest energy eigenvalues we construct the complete ortho-normal basis system by distributing N electrons within the M energetically lowest one-electron states. The rank $r(H)$ of the Hamiltonian matrix in the basis set of the N electron Slater determinants is given by the binomial coefficient

$$r(H) = \binom{2M}{N}.$$

Most of the results presented in the following section are obtained by restricting $M \leq 7$ for practical reasons, and since it was found that the lowest eigenvalue was sufficiently insensitive to M for small particle numbers ($N \leq 3$).

The matrix contains only a small fraction of non-vanishing off-diagonal elements (1...10%, depending on the values of M , and N). Nevertheless, as $r(H)$ is of the order of a few thousands a considerable amount of computing time is used for setting up the Hamiltonian matrix. An economic procedure to generate the non-vanishing matrix elements was found by starting from the complete basis corresponding to $(N-2)$ electrons. Applying two creation operators generates an N electron state (with the proper sign). It corresponds to a certain row of the Hamiltonian matrix. Creating two particles in two different (or same) one-electron states generates another N electron state identifying a certain column. Independent summation over all pairs of possible creations, and repeating the procedure for all $(N-2)$ particle states leads eventually to the complete occupation of the Hamiltonian matrix. The method is equivalent to a separate treatment of (i) the diagonal elements, (ii) matrix elements between states differing only in one excitation, (iii) in two excitations, and (iv) the vanishing matrix elements. The advantage of our method is that by construction only non-zero matrix elements are treated.

We have diagonalized matrices with $r(H)$ up to 3000. The accessible dimension of the matrix could be increased further by using recursive Lanczos procedures.

As one of the most stringent tests of the program the property of particle-hole symmetry was verified.

Defining the hole operators

$$b_{n\sigma} \equiv c_{n-\sigma}^\dagger, \quad b_{n\sigma}^\dagger \equiv c_{n-\sigma} \quad (18)$$

which fulfill the anti-commutation relations

$$[b_{n\sigma}, b_{n'\sigma'}^\dagger]_+ = \delta_{nn'} \delta_{\sigma\sigma'}, \quad (19)$$

one can show that

$$\begin{aligned} & \sum_{n_1, n_2, n_3, n_4, \sigma_1, \sigma_2} V_{n_4 n_3 n_2 n_1} c_{n_4 \sigma_1}^\dagger c_{n_3 \sigma_2}^\dagger c_{n_2 \sigma_2} c_{n_1 \sigma_1} \\ &= \sum_{n_1, n_2, n_3, n_4, \sigma_1, \sigma_2} V_{n_4 n_3 n_2 n_1} b_{n_4 \sigma_1}^\dagger b_{n_3 \sigma_2}^\dagger b_{n_2 \sigma_2} b_{n_1 \sigma_1} \\ & - U + D \end{aligned} \quad (20)$$

with the operators

$$U \equiv 2 \sum_{n_1, n_4, \sigma} [\sum_n (2 V_{n_4 n n n_1} - V_{n_4 n n_1 n})] b_{n_4 \sigma}^\dagger b_{n_1 \sigma} \quad (21)$$

$$D \equiv 2 [\sum_{n, n'} (2 V_{n n' n' n} - V_{n n' n n'})] 1. \quad (22)$$

The Hamiltonian matrix for N particles in M states must be identical to the one for $2M - N$ particles in M states when simultaneously a potential contribution $-U$ and a diagonal energy D are added.

4. The results

Including the electron-electron interaction the energy spectrum becomes extremely complicated as compared to the non-interacting case. First we consider the behavior of the ground state energy.

4.1. Ground state-energy

Figure 5 shows the ground state energy for $N=2$ for $L=1890 a_0$ as a function of γ . It is obvious that the limit of $\gamma \rightarrow 0$ is well-defined since the energy becomes independent of γ even on the scale of the one particle energy level differences, although each of the Hamiltonian matrix elements increases strongly with decreasing γ .

Figure 6 shows the ground state energy per particle multiplied by the length of the system versus L for different electron numbers, N , without taking into account the background potential. The curve for $N=1$ reflects the behavior of the contribution of the kinetic energy. Significant deviations from the Coulombic $1/L$ behavior of the ground state energy when L is decreased occur at $L \approx 300 a_0$. This is much larger than one would expect from the naive argument comparing kinetic and potential energy. We observed that there is an additional repulsive contribution to the energy which is due to the

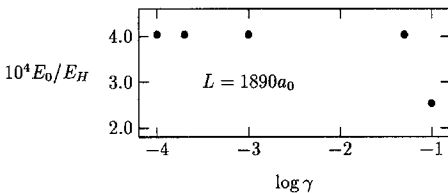


Fig. 5. Ground state energies for $N=2$ electrons in the M energetically lowest single particle states for a system length $L=1890 a_0$ as a function of the parameter γ which describes the lateral extend of the single particle wave functions

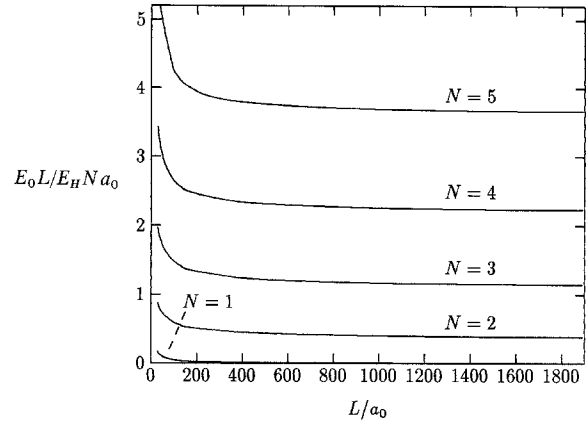


Fig. 6. Ground state energy E_0/N per particle multiplied by the system length L in atomic units for the electron numbers indicated. The background potential is not included. The constancy of the curves for $L \geq 500 a_0$ indicates the expected Coulombic $1/L$ dependence

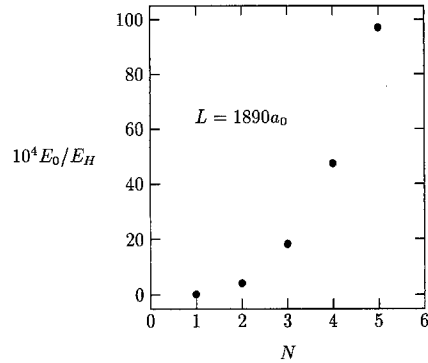


Fig. 7. Ground state energy of E_0 of N electrons in atomic units as a function of the electron number for $L=1890 a_0$. The background potential is not included

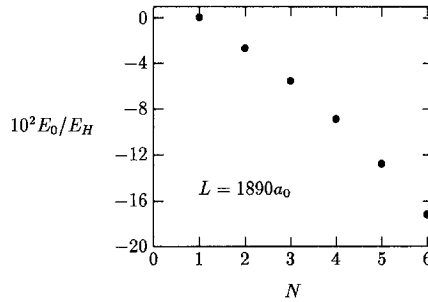


Fig. 8. Ground state energy E_0 in atomic units versus electron number N including the influence of the background potential for $L=1890 a_0$

fact that the electrons are in a state that extends over the whole system length.

Figure 7 shows the ground state energy as a function of the particle number. The more than linear increase of the energy per particle is possibly due to the restriction $M \leq 7$.

Without background the energy of the system is increasing with the number of the electrons due to Coulombic repulsion. Including the background potential is equivalent to introducing attractive forces that lead to

a decrease of the ground state energy when N is increased. This is shown in Fig. 8.

Since the ground state energy is dominated by the Coulomb interaction ($L \gg a_0$) the dependence on the electron number will be qualitatively the same if the width of the system becomes comparable to its length. It will also not depend on the exact shape of the confining potential. Of course, the absolute magnitudes of the ground state energies do depend on these features.

4.2. The energy spectrum of several electrons

The energy spectra for electron numbers $N \leq 5$ are shown in Fig. 9. Compared to the one-electron case, not only the total number of levels but also their density within certain energy regions are considerably increased.

For the low lying states three main properties are found. (i) There is a 2^N fold ground state multiplet with a considerably smaller energetic width than the gap immediately above. (ii) The number of the energetically different levels within the multiplet is equal to the number of irreducible representations of the rotation group of N coupled $1/2$ -spins. Each of the levels corresponds to a well defined total spin S , $0 \leq S \leq N/2$. (iii) The total ground state is spin polarized with a degeneracy $N + 1$.

Assuming that the ground state corresponds to a spatially oscillating density we can intuitively attribute the comparably large energy gap above the multiplet to the excitation of a vibrational mode with a finite frequency related to the Coulomb force between neighboring maxima of this "charge density wave". Correspondingly, the small energy splitting within the multiplet may be assigned to tunneling energies between the maxima. However, we are not sure whether or not these features would survive in the thermodynamic limit as there the vibrational gap should vanish due to the Goldstone theorem.

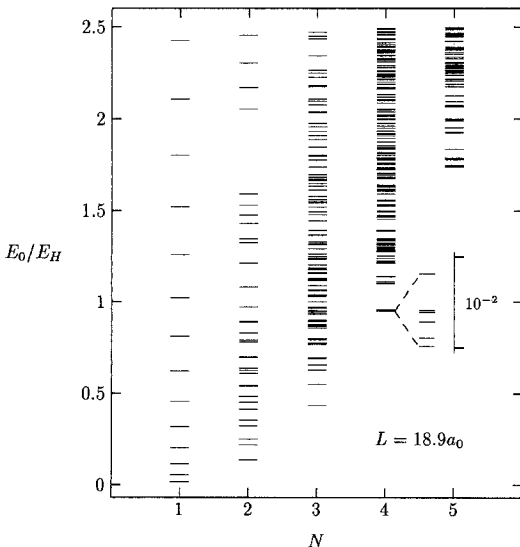


Fig. 9. Energy spectra for different electron numbers (in atomic units). The parameters are $\gamma = 2 \cdot 10^{-4}$, $M = 7$, $L = 18.9 a_0$. The background is not included. The energy of the ground state increases more than proportional to N^2 , due to quantum mechanical effects

5. Comparison with experiment

In this section the importance of the above results for the interpretation of the experimentally observed conductance oscillations in AlGaAs/GaAs samples [3] is discussed. Although we do not have a full theoretical formulation for the correlated tunneling process some qualitative understanding of the experiment has been achieved. Furthermore, an estimate of the energetic distance between the conductance peaks can be made.

We assume that the voltage applied to the gate (G in Fig. 1) is such that there are on the average N electrons within the region E between the two contacts (denoted by B in Fig. 1). We further assume that potential barriers represented by the constrictions isolate the interior of the island sufficiently well from the semi-infinite quasi-one dimensional systems attached to both sides in order to make tunneling improbable. This seems to be justified for the actual experimental situation since the temperature induced width of the conductance peaks is well described by the derivative of the Fermi function, and the contribution of tunneling to their zero-temperature width seems to be small. If the Fermi energy coincides with the ground state energy $E(N)$ of the N electrons when restricted to the island, the island will be quantum mechanically almost completely transparent. The conductance is at maximum.

We ask now how the conductance behaves when the gate voltage, i.e. the Fermi energy is changed. Varying the gate voltage only slightly, is equivalent to adding only a little amount of charge, say δq , to the island. There is no resonant island state available at the corresponding Fermi energy. The island is quantum mechanically opaque leaving the conductance exponentially small at $T=0$. Only if the variation of the gate voltage is large enough, such that the Fermi energy is close to the ground state of an integer number of electrons within the island the transmission probability through the entire "system" consisting of the (semi-infinite) "leads", the contacts, and the island the conductance can be high due to the formation of a resonant (multi-particle) state. Given a conductance peak at $E(N)$ the next resonance appears at the higher energy $E(N+1)$, the ground state of the $N+1$ electron state. The "activation energy" for the peaks is thus the energy required to add an additional electron to the correlated system of the N electrons already present between the barriers, at the least $\Delta = E_0(2) - E_0(1)$.

With the effective mass of GaAs, $m/m_0 = 0.067$, and for a system length of $L = 0.7 \mu\text{m}$, which compares roughly to the experimental value [20], we obtain $\Delta \approx 0.8 \text{ meV}$. In view of the rather crude model, this can be considered as consistent with the previous estimates of 0.5 meV based on the evaluation of the relation between the gate voltage and the chemical potential, and the observed temperature dependence of the shape of the conductance peaks [3].

Without taking into account the exchange terms properly, the magnitude of the activation energy would be an order of magnitude larger. This indicates the importance of the above mentioned compensation effect be-

tween Coulomb and exchange terms for the understanding of the experimental situation.

Many of the features seen in the experiment, as, for instance, the periodicity of the conductance resonances and their lineshapes, can also be understood by using the Coulomb blockade model, modified to take into account the discreteness of the one-electron energy levels [25]. However, as the exchange interaction term is not included in this model, no statement about the behavior of the spins of the electrons can be made. Our present microscopic treatment can clarify the range of validity of the Coulomb blockade model.

In the arguments used above we have assumed that the change in the background contribution to the energy is absorbed by the change in the gate voltage. We did also not consider the fact that the difference between the ground state energies increases with increasing electron number. It is likely that it is necessary to take into account the self-consistent adjustment of the charge distribution in the channel more realistically for a proper description of the experimental situation. The latter is also indicated by the observation that in the experiment the presence of about 100 electrons in the island is necessary before the conductance resonances can be observed.

6. Conclusion

We have presented the results of microscopic calculations concerning the electronic structure and the (linear) transport properties of quasi-one dimensional metallic systems interrupted by two constrictions that generate an almost isolated electronic island in between.

Neglecting electron-electron interaction it is possible to treat the resonant tunneling character of the conductance explicitly. However, there are serious quantitative, and qualitative discrepancies between the theoretical and the experimental results. Whereas the non-interacting theory predicts that two electrons should be necessary to generate a conductance resonance the experimental findings indicate that one electron is sufficient. In addition, the activation energy is an order of magnitude too small in the one-electron approximation, for the experimental sample geometry.

The exact calculation of the energy spectra of $N(N \leq 6)$ interacting confined electrons yielded as the main results the dominance of the Coulomb interaction for the geometrical dimensions of the samples used in the experiments, and a partial compensation of the Coulombic repulsion energy via exchange. A quantitative

estimate of the activation energy of the conductance peaks based on the microscopic calculation was found to be consistent with the experimental data.

The formulation of the transport theory for the interacting system taking into account the exact N -electron states is still to be done.

References

1. A collection of recent reviews concerning the quantum coherent transport phenomena that were discovered during the past decade can be found in: Quantum coherence in mesoscopic systems. Kramer, B. (ed.). New York: Plenum Press 1991
2. Field, S.B., Kastner, M.A., Meirav, U., Scott-Thomas, J.H.F., Antoniadis, D.A., Smith, H.I., Wind, S.J.: Phys. Rev. **B42**, 3523 (1990-II)
3. Meirav, U., Kastner, M.A., Wind, S.J.: Phys. Rev. Lett. **65**, 771 (1990)
4. Likharev, K.K.: IBM J. Res. Devel. **32**, 144 (1988)
5. Zant, H.S.J. van der, Geerligs, L.J., Mooij, J.E.: In Ref. 1, p. 511
6. Landauer, R.: Philos. Mag. **21**, 863 (1970); for a review see Landauer, R.: Localization interaction, and transport phenomena. In: Springer Series in Solid State Sciences. Kramer, B., Bergmann, G., Bruynseraede, Y. (eds.), Vol. **61**, p. 38. Berlin, Heidelberg, New York: Springer 1985
7. Economou, E.N., Soukoulis, C.M.: Phys. Rev. Lett. **46**, 618 (1981)
8. Fisher, D.S., Lee, P.A.: Phys. Rev. **B23**, 6851 (1981); a derivation for the more general case of a sample with several probes was given by Stone, A.D., Szafer, A.: IBM J. Res. Devel. **32**, 384 (1988)
9. Büttiker, M., Imry, Y., Landauer, R., Pinhas, S.: Phys. Rev. **B31**, 6207 (1985)
10. Mašek, J., Kramer, B.: Z. Phys. B – Condensed Matter **75**, 37 (1989)
11. Kramer, B., Mašek, J.: In Ref. 1, p. 317
12. Fal'ko, V.I.: Europhys. Lett. **8**, 785 (1989)
13. Washburn, S.: In Ref. 1, p. 341
14. Averin, D.V., Schön, G.: In Ref. 1, p. 531
15. Meir, Y., Wingreen, N.S., Lee, P.A.: Phys. Rev. Lett. **66**, 3048 (1991)
16. Prange, E.R., Girvin, S.M. (eds.): The quantum hall effect. Berlin, Heidelberg, New York: Springer 1987
17. Maksym, P.A., Chakraborty, T.: Phys. Rev. Lett. **65**, 108 (1990)
18. Merkt, U., Huser, J., Wagner, M.: Phys. Rev. **B43**, 7320 (1991)
19. Kawabata, A.: Solid State Commun. **32**, 893 (1979)
20. McEuen, P.L., Foxman, E.B., Meirav, U., Kastner, M.A., Meir, Y., Wingreen, N.S., Wind, S.J.: Phys. Rev. Lett. **66**, 1926 (1991)
21. MacKinnon, A.: Z. Phys. B – Condensed Matter **59**, 385 (1985)
22. Schweitzer, L., Kramer, B., MacKinnon, A.: J. Phys. **C17**, 4111 (1984)
23. Pines, D.: Elementary excitations in solids. New York: Benjamin 1964
24. Löwdin, P.O., Pollman, B.: Molecular orbitals in chemistry, physics and biology. New York: Academic Press 1964
25. Beenakker, C.W.J.: Phys. Rev. **B44**, 1646 (1991)